Supporting Information

Effect of Anatase crystal orientation on the photoelectrochemical performance of anodic TiO_2 nanotubes

Próspero Acevedo-Peña*[,a], Federico González[a], Gonzalo González[b] and Ignacio González[a]

[a] *Universidad Autónoma Metropolitana-Iztapalapa, Av. San Rafael Atlixco 186. Col. Vicentina, 09340, Ciudad de México, D.F. (México).*

[b] *Instituto de Investigaciones en Materiales, Universidad Nacional Autónoma de México, Circuito Exterior S/N, A.P. 70-360, Ciudad de México, D.F. (México).*

TiO_2 nanotube film characterization

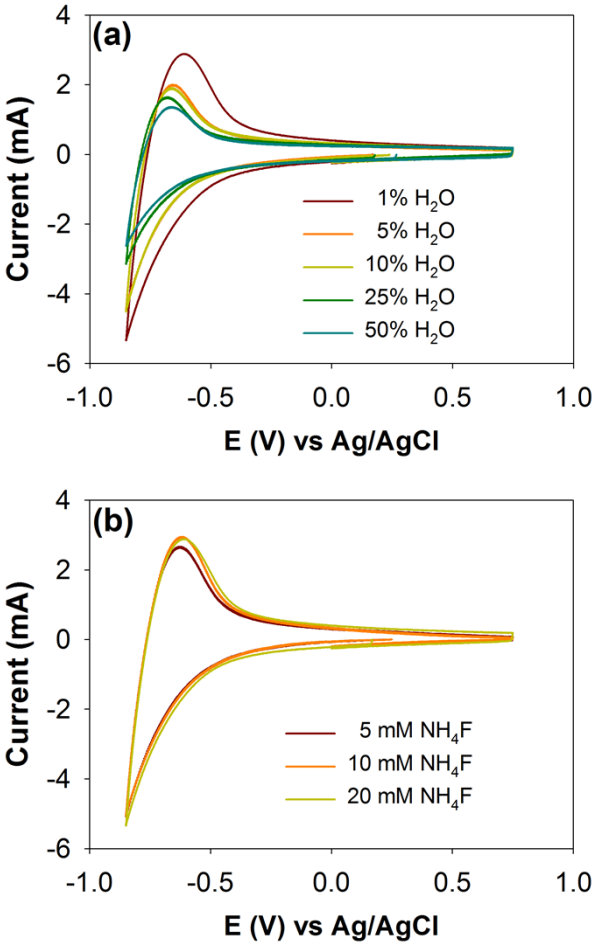

Figure S1. Voltammetric behavior ($v = 20$ mVs^{-1}) in a 0.1 M $HClO_4$ electrolyte, of the TiO_2 films grown at 30 V during 2 h in: (a) x M NH_4F in ethylene glycol (1%H_2O), and (b) 0.20 M NH_4F in ethylene glycol (x% H_2O).

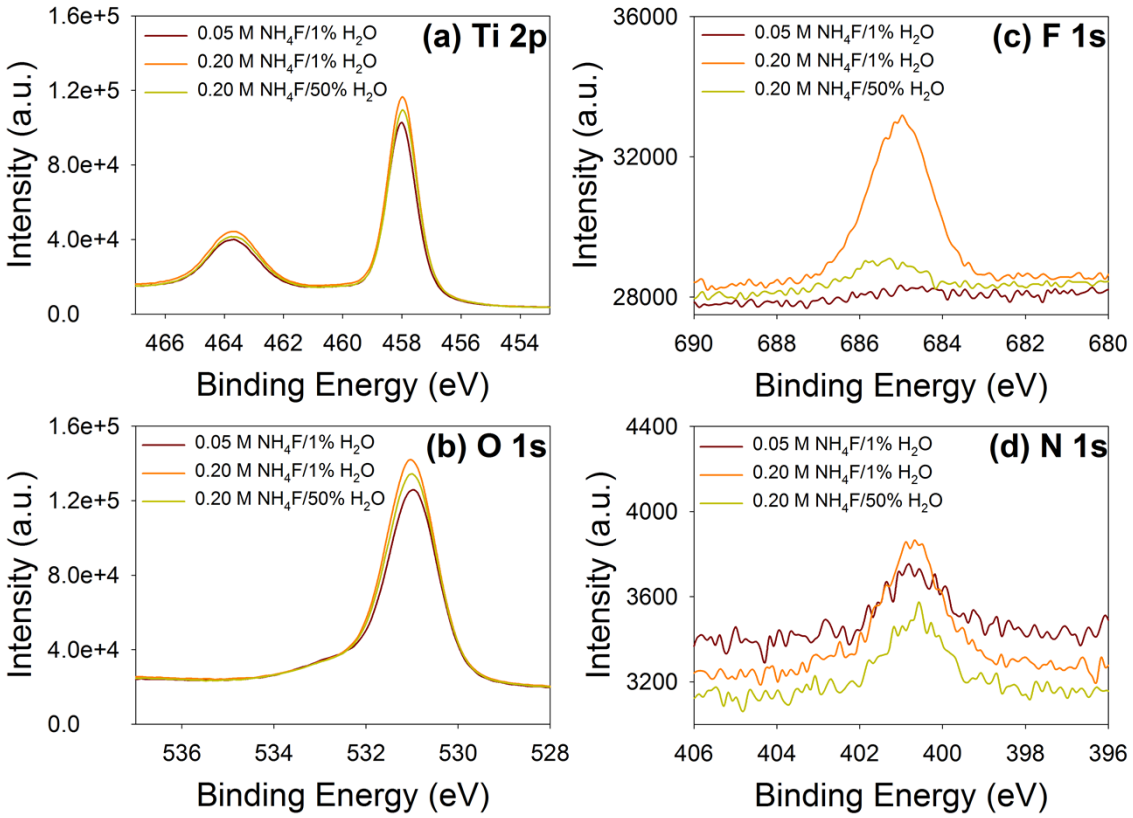

Figure S2. XPS spectra for (a) Ti_{2p}, (b) O_{1s}, (c) F_{1s} y (d) N_{1s}, measured for the films grown at 30 V during 2 h in (—) 0.05 M NH_4F in Ethylene glycol (1% H_2O), (—) 0.20 M NH_4F in ethylene glycol (1% H_2O) and (—) 0.20 M NH_4F in ethylene glyol (1% H_2O), and heat treated at 450°C (10°Cmin^{-1}) for 30 min. Each spectrum is the average of three measurements carried at different zones of the sample.

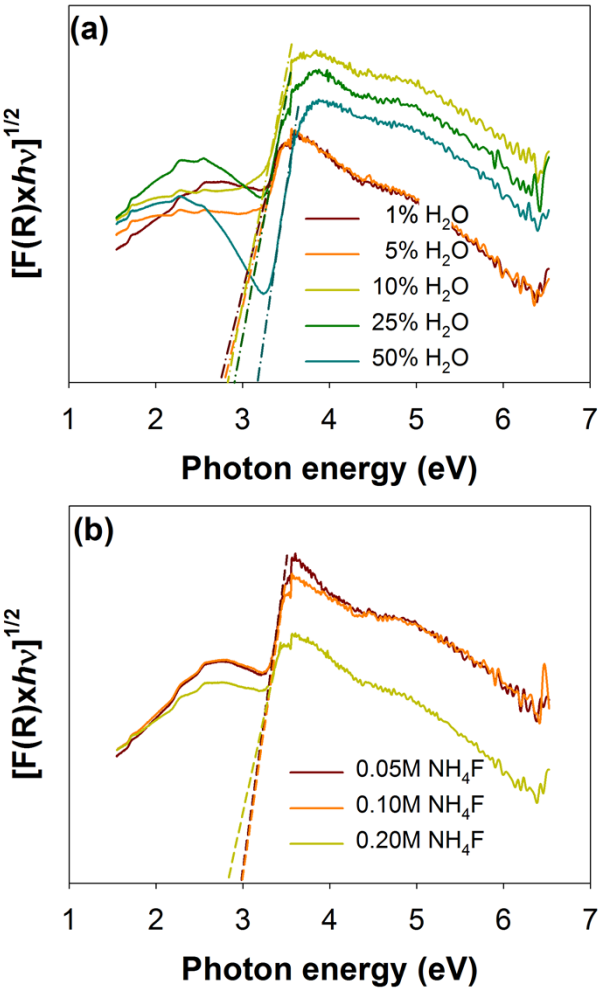

Figure S3. Graphical representation of modified Kubelka–Münk function for indirect allowed transitions, for the TiO_2 films grown at 30 V during 2 h in: (a) *x* M NH_4F in ethylene glycol (1%H_2O), and (b) 0.20 M NH_4F en ethylene glycol (*x*% H_2O).

Tabla 2. Dependance of E_g with the bath composition employed to grown the TiO_2 films by anodization at 30 V during 2 h.

[NH_4F] (M)	**%H_2O**	**E_g (eV)**
0.05	1	3.0
0.10	1	3.0
0.20	1	2.7
0.20	5	2.8
0.20	10	2.8
0.20	25	2.9
0.20	50	3.2

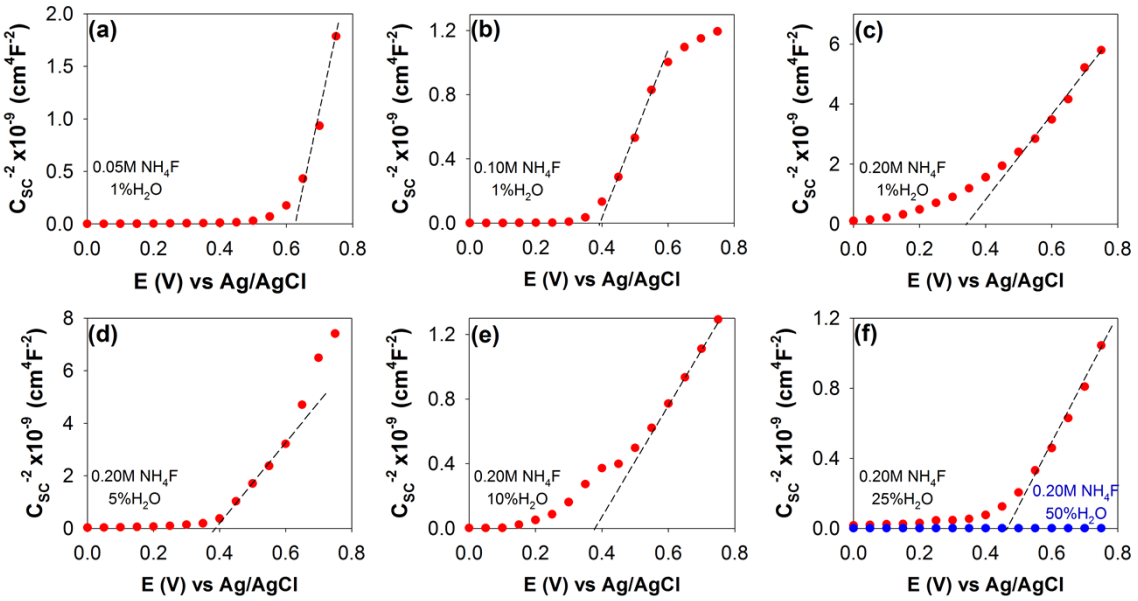

Figure S4. Mott-Schottky plots potentiostatically obtained in a 0.1 M $HClO_4$ electrolyte, for the TiO_2 films grown at 30 V during 2 h in different anodizing baths: (a) 0.05 M NH_4F, (b) 0.10 M NH_4F, (c) 0.20 M NH_4F in ethylene glycol with 1% H_2O, and 0.20 M NH_4F in ethylene glycol with (d) 5% H_2O, (e) 10% H_2O, and (f) 25% and 50% H_2O. Dashed lines indicate the linear zone in which the semiconducting properties were estimated.

Table S1. Semiconducting properties (N_d and E_{fb}) measured in a 0.10 M $HClO_4$ electrolyte, for the heat-treated TiO_2 films grown at 30 V during 2 h in different anodizing baths based in ethylene glycol.

[NH_4F] (M)	**%H_2O**	**$N_d \times 10^{-20}$ (cm^{-3})**	**E_{fb} (V vs Ag/AgCl)**
0.05	1	2.1	0.62
0.10	1	6.2	0.38
0.20	1	739.3	0.37
0.20	5	200.4	0.38
0.20	10	8.4	0.37
0.20	25	8.5	0.45

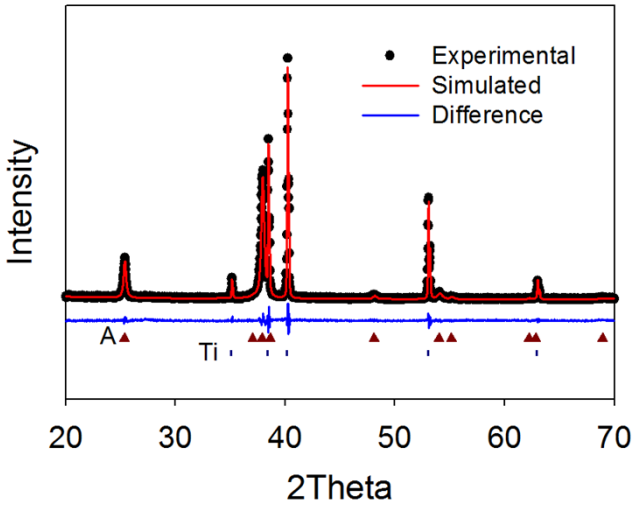

Figure S5. Rietveld refinement plot of the film growth at 30 V during 2 h and heat treated at 450 °C, in an electrolyte 0.05 M NH4F in etileneglycol (1% H2O). The points and the upper solid line correspond to the experimental and calculated data, respectively; the lower solid line is the difference between them. Upper marks correspond to anatase, whereas the lower ones correspond to metallic titanium.

Corrected $TC_{(004)}$ estimation

Further than texture, the most significant difference of the X-ray diffracted signal in the Bragg Brentano geometry between anatase in a powder form, containning isotropic particles, and anatase in nanotube shape, is that due to the shape anisotropy of the last one, it may induces intensity and peak broadening (narrowing) variations as a function of the nanotube tilting angle ψ with respect to the surface normal. Actually, in the case of a nanotube, in order to establish the number of planes that contributes to the diffraction in this direction it should be considered the effective size l_{eff} along the surface normal. l_{eff} is the projection of the nanotube long axis l on the surface normal direction bounded, at high inclination angles ($\psi > tan^{-1}(l/w)$), by the cross section w (wall thickness of nanotubes), equation (S1):

$$l_{eff} = l\ max[\cos\psi, A_r \sin\psi];\ A_r = w/l. \quad \text{(S1)}$$

Since the diffracted intensity scales with the square of this length, the shape related correction factor for the intensity is

$$f_{shape\ corr} = max\ [\cos^2\psi, A^2{}_r \sin^2\psi] \quad \text{(S2)}$$

where A_r is the aspect ratio of the nanotube. Assuming a *c*-oriented nanotube, the correction factor in Eq. (S2) is maximal for (00*l*) reflections and minimal for (*hk*0) ones. In the case of isotropic particles, the hollow cylinder model of Eq. (S1) no longer applies and the correction for all reflections is 1.

From Table 1, it is evident that *l* is two orders of magnitude greater than *w*, so $A_r \sin\psi > \cos\psi$ for $\psi \sim 90°$. Thus, in Eq. (S3), the (*h00*) –or (*0k0*)- reflections are the only ones for which l_{eff} is calculated as $lA_r \sin\psi_{h00}$, but $lA_r \sin\psi_{h00} \sim lA_r \sim 11$ nm. Similarly, in Eq. (S2), the (*h00*) –or (*0k0*)- reflections are the only ones for which $f_{shape\ corr}$ is calculated as $A^2_r \sin^2\psi_{h00}$. In this case $A^2_r \sin^2\psi_{h00} \sim A^2_r \sim 0$, since $A_r \sim 10^{-2}$. In fact, for the 10 reflections considered, only the (002) one is in that condition.

$$TC_{(004)} = \frac{10}{\sum f_{corr}} = 2.41 \quad \text{(S3)}$$

Table S1. Correction factor associated with the nanotubular morphology for each Bragg reflection of the anatase. The Ψ value corresponds to the angle between each crystalline plane in the anatase structure and its (001) plane.

(hkl)	2θ (°)	Ψ (°)	f_{corr}
101	25.30	68.3	0.137
103	36.95	39.9	0.588
004	37.81	0	1.000
112	38.56	60.6	0.241
200	48.02	90	0
105	53.91	26.7	0.798
211	55.04	79.9	0.031
213	62.09	61.9	0.222
204	62.68	51.5	0.388
116	68.78	30.6	0.741